$\pi^+ d \rightarrow \pi^+ pn$ reaction as a test of relativistic Faddeev theories: Differential cross section

W. Gyles, E. T. Boschitz, H. Garcilazo,* W. List, E. L. Mathie,† C. R. Ottermann, G. R. Smith,‡ and R. Tacik
Kernforschungszentrum Karlsruhe, Institut für Kernphysik and Institut für Experimentelle Kernphysik der Universität Karlsruhe, 7500 Karlsruhe, Federal Republic of Germany

R. R. Johnson
TRIUMF, University of British Columbia, Vancouver, British Columbia, Canada V6T 2A3
(Received 30 July 1985)

Three-fold differential cross sections $\sigma(\theta_\pi, \theta_p, P_p)$ have been measured in a kinematically complete experiment over a large region of phase space at 228 and 294 MeV incident pion energy. The data are compared with predictions from a relativistic Faddeev calculation. Excellent agreement is found over most of the phase space. From this good agreement between theory and experiment there appears to be no need for the inclusion of nonconventional dynamics, such as the excitation of dibaryon resonances.

I. INTRODUCTION

The systematic experimental investigation of the πNN system is of foremost importance because it is a three-body system for which one can hope to obtain reliable theoretical predictions. At present these predictions are based on conventional meson exchange approaches; in the future they will possibly be in the framework of a bag model. For several years it has been recognized that the most stringent test of advanced unified three-body theories is the simultaneous comparison of the theoretical predictions with many measured observables in all reaction channels of the πNN system. In this system the following reaction channels are coupled together:

$$\begin{array}{ccccc} \mathrm{NN} \rightarrow \mathrm{NN} & \longleftrightarrow & \pi\mathrm{d} \leftarrow \pi\mathrm{d} \\ \searrow & \pi\mathrm{NN} & \swarrow \end{array} .$$

Experimentally, the elastic nucleon-nucleon channel and the pion absorption–production ($pp \leftrightarrow \pi^+ d$) channel are the only ones which have been studied thoroughly up to proton energies of 1 GeV.[1–4] Regarding the πd elastic scattering reaction, data exist only for the differential cross section and the vector analyzing power,[5–8] as well as a few controversial measurements of the tensor analyzing power.[9–12] More polarization measurements are planned at SIN and TRIUMF. For the inelastic channels NN$\rightarrow\pi$NN (Refs. 13–18) and πd$\rightarrow\pi$NN (Refs. 19 and 20) systematic measurements only started a few years ago due to the greater difficulty of providing kinematically complete measurements in reactions with a three-body final state.

So far there is no calculation of all five channels simultaneously. Much work has been done describing the individual channels and, in some of the three-body calculations, providing predictions for two or even three channels at the same time.[21] In trying to reproduce the experimental data great difficulties are encountered in the pp$\rightarrow\pi$d (Refs. 22 and 23) and NN$\rightarrow\pi$NN reactions.[24] This indicates that some important part of the reaction dynamics may be missing. It has been suggested that this could be related to the formation and the decay of dibaryons, but so far there is no clear evidence to support such a hypothesis.

The πd breakup channel has not yet been put to a severe theoretical test, due to lack of comprehensive data. This reaction is very interesting, however, because it not only leads to the same final state as the $pp \rightarrow \pi^+ pn$ reaction, but it also has the advantage that the partial width of a possible dibaryon resonance decay in the NΔ (1232) channel, i.e., $B^2 \rightarrow N\Delta \rightarrow \pi pn$, is significantly larger than those in the $B^2 \rightarrow pp$ and $B^2 \rightarrow \pi d$ channels. This has been shown by Araki *et al.*[25] within a Faddeev formalism, by Duck and Umland[26] within a perturbation calculation, and by Grein *et al.*[27] within a bag model calculation.

The deuteron breakup reaction was investigated for the first time by Bayukov *et al.*[28,29] with 1 GeV/c negative pions. The scattered pions were detected in the angular region $\theta_\pi = 17°–23°$ by a magnetic spectrometer, the recoiling protons by a range spark chamber at 70°. In the region of small momentum transfer to the neutron ($q < 80$ MeV/c) good agreement between the data and the model of quasielastic knockout was obtained. At larger values for q the neutron momentum distribution differed appreciably from predictions based on this model, but good agreement was obtained by including the final state interaction between the proton and neutron.

At lower pion momenta (371, 438, and 552 MeV/c) Dakhno *et al.*[30–34] studied the reaction $\pi^- d \rightarrow \pi^- pn$ in detail with a deuterium bubble chamber. The data were interpreted in terms of quasifree scattering and rescattering of πN and NN. Quasifree scattering was considered to be dominant. Although the authors aimed for good statistical precision, this is necessarily limited with this experimental technique and, therefore, the data are presented as double rather than triple differential cross sections. This greatly reduces the sensitivity for comparison with a sophisticated calculation.

Kinematically complete measurements of the $\pi^{\pm}d \rightarrow \pi^{\pm}pn$ reaction were performed by Hoftiezer *et al.* at 340 MeV/c.[19,20] Data of high statistical precision were obtained at 11 angle pairs. The pions were detected by a time-of-flight technique, the protons by a magnetic spectrometer. The data were compared with a distorted-wave impulse approximation (DWIA) calculation, including some corrections for the NN and the πN final state interactions. It was found that the impulse approximation provides a qualitative description of most of the data. The shape of the differential cross section as a function of the proton momentum is generally reproduced, but the magnitude of the calculated cross section sometimes differs from the data by a factor of 3. The authors found that the only correction to the impulse approximation that is significant at the lowest spectator neutron momenta is multiple scattering in the entrance channel. Corrections due to NN and πN final state interactions were found to be insignificant here. For neutron momenta above about 40 MeV/c drastic discrepancies from the DWIA were observed. They could be remarkably reduced by adding a $J^{\pi}=2^{+}$ NΔ "dibaryon" resonance amplitude to an impulse approximation background. However such a correction most likely only accounts for the inadequacy of the DWIA calculation.

Stimulated by this experimental work, relativistic Faddeev calculations have been performed by Matsuyama[35] and by Garcilazo.[36] Matsuyama found that in the region which corresponds to small neutron recoil momentum the impulse contribution is dominant and determines the gross structure of the cross sections, but the higher order processes also contribute appreciably in some cases. The calculation reproduces the experimental data within a factor of 2. The calculation of Garcilazo on the other hand reproduces the proton momentum distribution much better, particularly in the region where the mass of the $\pi^{+}p$ subsystem is near the Δ^{++} mass. However, there are also severe discrepancies between this calculation and the data of Hoftiezer *et al.* in the region of low proton momenta (the kinematical region far away from the quasifree scattering).

Recently Goetz *et al.*[37] measured the $\pi^{-}d \rightarrow \pi^{-}pn$ reaction at 150 MeV detecting the pions with a spectrometer at 77.5° and 90° and the neutrons (protons) at 40°±9.5° with a large area neutron (proton) detector. The data, presented, as double differential cross sections $d^2\sigma/d\Omega_{\pi}d\Omega_{N}$ and $d^2\sigma/d\Omega_{\pi}dT_{\pi}$, were compared with an impulse approximation calculation. Both the ratio of neutrons to protons detected and the low energy side of the pion energy spectra show significant discrepancies from this simple model. However, as noted earlier, the sensitivity of the comparison to a sophisticated calculation is largely lost, due to the integration of the cross sections over the momentum or the angles, respectively.

Considering the existing situation, it is clear that comprehensive measurements of this reaction channel are badly needed and should be compared with a refined three-body calculation. The data of Hoftiezer *et al.* should be checked using a different detection technique, particularly in the region of largest departures from the Faddeev predictions. The data should also be extended to the region as far away from the quasifree scattering as possible, in order to provide a stringent test of relativistic Faddeev theories. If there is any hope of detecting dibaryon signals then it is most likely in these kinematical regions where the principal diagrams no longer dominate.

This work is part of a program to study the differential cross section and the vector analyzing power in the $\pi^{+}d \rightarrow \pi^{+}pn$ reaction. The first results have been published recently.[38] In this paper we compare new relativistic Faddeev calculations with extensive cross section measurements at two pion energies. In the following paper we report the measurements of the vector analyzing power for this reaction at three energies at and above the (3,3) resonance.

II. THEORY

A. General remarks

In recent years pion-deuteron scattering has become a favorite testing ground for the various theories of the relativistic three-body problem. The so-called relativistic Faddeev equations were developed following a suggestion of Blankenbecler and Sugar,[39] by Alessandrini and Omnes,[40] and by Freedman, Lovelace, and Namyslowsky,[41] although the version that is always used in practice is that put in final form by Aaron, Amado, and Young[42] (which we will refer to from now on as AAY). This theory has been applied with considerable success by Kloet *et al.*[43–46] to describe nucleon-nucleon scattering above the pion production threshold. Similarly it was also the AAY theory that was used in all the early attempts to describe the πd system,[47–53] where only the observables of the elastic channel were calculated. This has been an unnecessary restriction of the AAY theory, since as a Faddeev theory it satisfies three-body unitarity, which means that the solution of the integral equations which describes the elastic channel gives also the cross sections for all the inelastic channels. Of the inelastic channels, by far the largest one in the resonance region is the breakup reaction $\pi d \rightarrow \pi np$ (it is even larger than the elastic one by roughly a factor of 2). It is therefore important to use this reaction as a test for the AAY theory.

Another development, completely independent of the AAY theory, came as a result of the realization by Mizutani and Koltun[54] that, due to the pion absorption by the deuteron, in addition to intermediate πNN states one can have also NN states. Thus, the Hilbert space of the problem consists of two sectors, the two-body NN sector and the three-body πNN sector. These two sectors are coupled together through the mechanism of absorption and emission of a pion by a single nucleon. The Mizutani-Koltun idea has led to the development of the so-called NN-πNN theory by Avishai and Mizutani[55] and independently by Blankleider and Afnan.[56] This new theory differs from the old AAY theory only in the treatment of the pion-nucleon P_{11} partial wave. This partial wave is treated in the AAY theory in exactly the same way as any other pion-nucleon partial wave. The NN-πNN theory on the other hand, splits the P_{11} amplitude into the sum of two terms, called the pole and nonpole parts, which are then used independently as separate input elements in the three-body equations. Thus, even though the P_{11} amplitude in the physical region is very small, it turns out that the pole and nonpole parts are both large (but of opposite sign), so that the effect of the P_{11} channel in the NN-πNN theory is very large. This is in total contradiction with the small effects that this channel has in the AAY theory.

It is interesting that when the predictions of the NN$\to\pi$NN theory by three different groups[56–58] were compared with tensor polarization measurements by Ungricht *et al.*,[9,10] they were in total disagreement with the data (and also with one another). However, a calculation,[59] based on the AAY theory, was able to explain these tensor polarization data and also the vector polarization data measured by Smith *et al.*[8] An explanation of these results, which has been offered by Garcilazo,[59] is that the old AAY theory is almost right because the influence of the pion absorption channel on the other channels is quite small; the pion absorption cross section comprises only about 5% of the total cross section. In order to support this explanation he calculated the pion absorption cut and studied its influence on the differential cross section and reaction parameters, which was indeed found to be essentially negligible. The pion absorption cut is the contribution of the pion absorption channel to the three-body-unitarity discontinuity relations and is essentially model independent and therefore it is the same in both theories. Thus it was concluded in Refs. 9 and 59 that the large effects obtained in the NN-πNN theory were most likely spurious.

We have now applied the model of Refs. 53, 60, 36, and 59 to our new extensive πd breakup measurements, as a further test of the AAY theory. We will be anxious to see the corresponding predictions from the three groups representing the NN-πNN theory.

We solve the AAY equations using as input the six S and P wave pion-nucleon channels and the two S-wave nucleon-nucleon channels by means of separable T matrices. For the pion-nucleon subsystem we choose them as

$$t_l(p,p';s)=p^l\frac{g(p)}{g(p_0)}\tau_l(s)p'^l\frac{g(p')}{g(p_0)}\ , \tag{1}$$

with

$$s=(\sqrt{M^2+p_0^2}+\sqrt{\mu^2+p_0^2})^2\ , \tag{2}$$

$$g(p)=1/(\alpha^2+p^2)\ , \tag{3}$$

$$\alpha=1\ \mathrm{GeV}/c\ . \tag{4}$$

The amplitudes $\tau_l(s)$ are constructed directly from the experimental pion-nucleon phase shifts, while the contribution of the pion absorption cut is added as described in Ref. 59. For the nucleon-nucleon subsystem, we apply the unitary pole approximation to the solution of the Paris potential[61] for the ${}^3S_1$-${}^3D_1$ bound state and ${}^1S_0$ antibound state. These two poles of the nucleon-nucleon amplitude are very important for the description of the breakup reaction, since they dominate the cross section in the so-called "final-state-interaction region," where the two nucleons come out very close to each other. In addition, this choice guarantees that our initial state deuteron wave function is the Paris wave function[61,62] which gives a very good description of the deuteron electromagnetic form factor.[63] We treat relativistically both the space and the spin variables, by the use of Wick's three-body helicity formalism.[64] We solve the integral equations along the real axis by the method of the Padé approximants using a variable 44-point Gaussian mesh and regularizing the integral equations by subtraction of the three-body logarithmic singularities of the kernel. We estimate the numerical accuracy of our solutions at approximately 1%. We solved the integral equations for all values of the total angular momentum $J<6$ and used the impulse approximation for the remaining values up to $J=14$. The complete expressions for the differential cross section and vector analyzing power can be found in the following section.

B. Formalism

In general, given three particles of masses m_1,m_2,m_3, spins $\sigma_1,\sigma_2,\sigma_3$, and isospins τ_1,τ_2,τ_3, we can represent a plane-wave state by means of Wick's three-body helicity states.[64]

$$|q_ip_i;\alpha_i\rangle=|q_ip_i;JMj_im_i\nu_i\lambda_j\lambda_k;TM_TT_i\rangle\ , \tag{5}$$

where p_i is the magnitude of the relative momentum between particles j and k measured in the c.m. frame of the pair, and q_i is the magnitude of the relative momentum between the pair jk and the particle i measured in the three-body c.m. frame. The discrete quantum numbers α_i are the helicities λ_j and λ_k of particles j and k which are measured in the two-body c.m. frame, j_i which is the total angular momentum of the pair jk and m_i its helicity, the

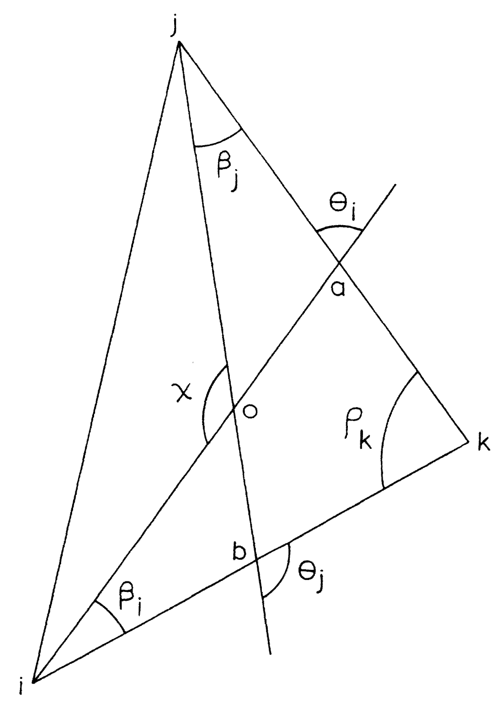

FIG. 1. The Wick triangle. The variables are defined in the text.

helicity ν_i of particle i, the total angular momentum, J, and its Z component M (all of which are measured in the three-body c.m. frame), T_i which is the isospin of the pair jk, T the total isospin, and M_T its Z component.

If we assume that the particle 1 is the pion and particles 2 and 3 the two nucleons, then the relativistic Faddeev equations for pion-deuteron scattering are written in terms of the basis states (5), as[60]

$$\langle q_i p_i;\alpha_i \mid T_i \mid \phi^J_{M_0}\rangle = (1-\delta_{i1})\langle q_i p_i;\alpha_i \mid t_i \mid \phi^J_{M_0}\rangle + \sum_{j\neq i}\sum_{\alpha_i' \alpha_j}\int q_i'^2 dq_i' p_i'^2 dp_i' q_j^2 dq_j p_j^2 dp_j J_i(p_i' q_i') \times J_j(p_j q_j)\langle q_i p_i;\alpha_i \mid t_i \mid q_i' p_i';\alpha_i'\rangle \frac{2W(p_i' q_i')}{W^2(p_i' q_i')-S-i\epsilon} \times \langle q_i' p_i';\alpha_i' \mid q_j p_j;\alpha_j\rangle\langle q_j p_j;\alpha_j \mid T_j \mid \phi^J_{M_0}\rangle , \tag{6}$$

where S is the invariant mass squared of the three-body system, $\phi^J_{M_0}$ is the initial-state wave function of the system with total angular momentum J and helicity of the deuteron M_0, $J_i(p_i,q_i)$ is the Jacobian that transforms the three-body phase space from single-particle variables to the relative variables q_i and p_i, and it is given by

$$J_i(p_i q_i) = \frac{\omega(p_i)}{8W_i(p_i q_i)\omega_i(q_i)\omega_j(p_i)\omega_k(p_i)} , \tag{7}$$

$$\omega(p_i) = (m_j^2+p_i^2)^{1/2}+(m_k^2+p_i^2)^{1/2} , \tag{8}$$

$$W_i(p_i q_i) = [\omega^2(p_i)+q_i^2]^{1/2} , \tag{9}$$

$$W(p_i q_i) = (m_i^2+q_i^2)^{1/2}+[\omega^2(p_i)+q_i^2]^{1/2} . \tag{10}$$

The two-body scattering amplitudes t_i that appear in Eq. (6) are given by

$$\langle q_i' p_i';\alpha_i' \mid t_i \mid q_i p_i;\alpha_i\rangle = \delta_{J'J}\delta_{M'M}\delta_{j_i' j_i}\delta_{m_i' m_i}\delta_{\nu_i' \nu_i}\delta_{T'T}\delta_{M_T' M_T}\delta_{T_i' T_i}\frac{2\omega_i(q_i)}{q_i^2}\delta(q_i'-q_i)\langle p_i';\lambda_j'\lambda_k' \mid t_i^{j_i T_i}(s_i(q_i)) \mid p_i;\lambda_j\lambda_k\rangle , \tag{11}$$

where $s_i(q_i)$ is the invariant mass squared of the pair jk, which is given by

$$s_i(q_i) = S+m_i^2-2\sqrt{S}(m_i^2+q_i^2)^{1/2} . \tag{12}$$

The separable or isobar approximation for the two-body amplitudes takes in this formalism the form

$$\langle p_i';\lambda_j'\lambda_k' \mid t_i^{j_i T_i}(s_i) \mid p_i;\lambda_j\lambda_k\rangle = \sum_{L_i S_i} h^{L_i S_i j_i T_i}_{\lambda_j'\lambda_k'}(p_i')\tau_i^{L_i S_i j_i T_i}(s_i) h^{L_i S_i j_i T_i}_{\lambda_j \lambda_k}(p_i) , \tag{13}$$

where

$$h^{L_i S_i j_i T_i}_{\lambda_j\lambda_k}(p_i) = \left[\frac{2L_i+1}{2j_i+1}\right]^{1/2} C^{L_i S_i j_i}_{0,\lambda_j-\lambda_k} C^{\sigma_j\sigma_k S_i}_{\lambda_j,-\lambda_k} g_i^{L_i S_i j_i T_i}(p_i) , \tag{14}$$

and L_i and S_i are the usual orbital angular momentum and spin quantum numbers of the pair jk. The form factors $g_i^{L_i S_i j_i T_i}(p_i)$ as described in the previous section are taken to be the same for all pion-nucleon channels

$$g_i^{L_i S_i j_i T_i}(p_i) = \frac{1}{\alpha^2+p_i^2} , \tag{15}$$

with the range parameter $\alpha = 1$ GeV/c, while for the nucleon-nucleon channels we apply the unitary pole approximation to the ${}^3S_1$-${}^3D_1$ bound state and ${}^1S_0$ antibound state solutions of the Paris potential.[61]

The recoupling coefficients between states of type i and those of type j that appear in Eq. (6), are given as

$$\langle q_i' p_i';\alpha_i' \mid q_j p_j;\alpha_j\rangle = \delta_{J'J}\delta_{M'M}\delta_{T'T}\delta_{M_T' M_T}\delta[W(p_i' q_i')-W(p_j q_j)]H(1-\cos^2\chi) \times \frac{4\omega(p_i')\omega(p_j)}{p_i' q_i' p_j q_j}[(2j_i'+1)(2j_j+1)(2T_i'+1)(2T_j+1)]^{1/2} \times (-)^{\sigma_j-\nu_j+\sigma_k+\lambda_k+T_j+\tau_j-T} d^J_{m_j-\nu_j,m_i'-\nu_i'}(\chi) d^{j_i}_{m_i',\lambda_j'-\lambda_k'}(\theta_i) \times d^{j_j}_{m_j,\lambda_k-\lambda_i}(\theta_j) d^{\sigma_i}_{\nu_i'\lambda_i}(\beta_i) d^{\sigma_j}_{\nu_j,\lambda_j'}(\beta_j) d^{\sigma_k}_{\lambda_k,\lambda_k'}(\rho_k) W(\tau_j\tau_k T\tau_i;T_i T_j) , \tag{16}$$

where H is the step function, and the arguments of the rotation matrices are the angles of the Wick triangle shown in Fig. 1, where the distances θ_i and θ_j represent the velocities of particles i and j in the three-body c.m. frame, the distances aj and ak represent the velocities of particles j and k in the two-body c.m. frame of the pair jk, etc.

The solutions of the integral Eq. (6) describe all elastic and inelastic processes having the pion-deuteron system as the initial state. Thus, for example, the amplitude for pion-deuteron elastic scattering is given by

$$F_{M_f M_0} = \sum_J \eta_J^2 d^J_{M_0,M_f}(\theta_{\text{c.m.}}) \sum_{i=2,3} \langle \phi^J_{M_f} \mid T_i \mid \phi^J_{M_0} \rangle , \tag{17}$$

where

$$\eta_J = \left[\frac{2J+1}{4\pi} \right]^{1/2} , \tag{18}$$

and

$$\langle \phi^J_{M_f} \mid T_i \mid \phi^J_{M_0} \rangle = \sum_{\alpha_1 \alpha_i} \int q_1^2 dq_1 p_1^2 dp_1 q_i^2 dq_i p_i^2 dp_i J_1(p_1 q_1) J_i(p_i q_i) \langle \phi^J_{M_f} \mid q_1 p_1 ; \alpha_1 \rangle \langle q_1 p_1 ; \alpha_1 \mid q_i p_i ; \alpha_i \rangle \langle q_i p_i ; \alpha_i \mid T_i \mid \phi^J_{M_0} \rangle , \tag{19}$$

with the differential cross sections in the c.m. system given by

$$\frac{d\sigma}{d\Omega} = \frac{\pi^4}{S} \frac{1}{3} \sum_{M_0 M_f} \mid F_{M_f M_0} \mid^2 . \tag{20}$$

The amplitude for the pion-deuteron breakup reaction, on the other hand, is obtained from the solutions of Eq. (6), as

$$F_{\nu_2 \nu_3, M_0} = \sum_{i=1}^{3} \sum_{\substack{JMj_i m_i \\ \lambda_j \lambda_k}} \eta_J^2 \eta_{j_i} d^{\sigma_j}_{\nu_j \lambda_j}(\beta_j) d^{\sigma_k}_{\nu_k \lambda_k}(\beta_k) \mathscr{D}^J_{M_0, m_i - \nu_i}(\phi_{q_i}, \theta_{q_i}, \phi_{p_i}) d^{j_i}_{m_i, \lambda_j - \lambda_k}(\theta_{p_i}) \langle q_i p_i ; \alpha_i \mid T_i \mid \phi^J_{M_0} \rangle . \tag{21}$$

The rotation matrices $d^{\sigma_j}_{\nu_j \lambda_j}(\beta_j)$ and $d^{\sigma_k}_{\nu_k \lambda_k}(\beta_k)$ in Eq. (21) are the matrix elements of the unitary transformation that connects the helicities of particles j and k from the two-body c.m. frame to the three-body frame. The differential cross section in the laboratory frame is given by

$$\frac{d^3\sigma}{d\Omega_1 dk_2 d\Omega_2} = \frac{\pi^4 k_1^2 k_2^2}{6 q_{10} \sqrt{S}\, \omega_2 \mid \omega_3 k_1 - \omega_1 \hat{\mathbf{k}}_1 \cdot \mathbf{k}_3 \mid} \sum_{\nu_2 \nu_3 M_0} \mid F_{\nu_2 \nu_3, M_0} \mid^2 , \tag{22}$$

where $\mathbf{k}_1$, $\mathbf{k}_2$, and $\mathbf{k}_3$ are the laboratory momenta of the pion, proton, and neutron, respectively, and ω_1, ω_2, and ω_3 their energies, while q_{10} is the initial momentum of the pion in the c.m. frame. The vector analyzing power iT_{11} is given in terms of the amplitudes of Eq. (21) as

$$iT_{11} = \frac{\sqrt{6}}{\sum_{\nu_2 \nu_3 M_0} \mid F_{\nu_2 \nu_3, M_0} \mid^2} \text{Im}[F^*_{(1/2)(1/2),0}(F_{(1/2)(1/2),1} - F_{(1/2)(1/2),-1}) + F^*_{(1/2)-(1/2),0}(F_{(1/2)-(1/2),1} - F_{(1/2)-(1/2),-1})] \tag{23}$$

and the tensor analyzing power, T_{20}, as

$$T_{20} = \frac{\sqrt{2}}{\sum_{\nu_2 \nu_3 M_0} \mid F_{\nu_2 \nu_3, M_0} \mid^2} [\, \mid F_{(1/2)(1/2),1} \mid^2 + \mid F_{(1/2)-(1/2),1} \mid^2 + \mid F_{(1/2)(1/2),-1} \mid^2 + \mid F_{(1/2)-(1/2),-1} \mid^2 - 2 \mid F_{(1/2)(1/2),0} \mid^2 - 2 \mid F_{(1/2)-(1/2),0} \mid^2] . \tag{24}$$

III. EXPERIMENTAL TECHNIQUE

In order to perform a kinematically complete experiment for the pion deuteron breakup reaction, it is sufficient to specify the incident beam energy, the reaction angles of two of the final state particles, and the momentum of one of them. Since it was the purpose of this experiment to cover a wide region of phase space and maintain good statistical accuracy even in the kinematical regions where the cross section is very low, the use of a magnetic spectrometer was ruled out because of the limited solid angle. Instead we employed a multiple arm time-of-flight (TOF) spectrometer which has been described in earlier publications.[8] The experiment was performed in the $\pi M3$ area of the Swiss Institute for Nuclear Research (SIN). Protons were detected on one side of the beam in coincidence with pions on the other side. Particle types were identified by recording both time-of-flight and pulse height information. During the same experimental period πp and πd elastic scattering differential cross sections were measured[7] using the same apparatus with slightly enlarged proton detectors. These cross sections agree well with those of Bussey *et al.*[65] and Gabathuler *et al.*[5], respectively, within the experimental uncertainties of about 5%.

The total beam size at the target was 20×25 mm^2 FWHM. The accepted pion beam was defined by two scintillators $S1$ and $S2$ in coincidence. $S1$ was a small scintillator (10×15 mm$^2\times1$ mm thick) placed 10 cm in front of the target and $S2$ (40×100 mm$^2\times2$ mm thick) was placed 1.5 m upstream of the target. The coincidence condition was $\mathrm{BEAM}=S1\cdot\overline{S1}\cdot S2\cdot\overline{S2}\cdot\mathrm{rf}$, where $\overline{S1}$ and $\overline{S2}$ are veto signals from discriminators with thresholds set above the pion pulse height and below the pulse height for protons in the beam and rf is the cyclotron radio frequency signal. Most of the protons in the beam were removed by degrading their energy with 10 mm of graphite in the center of the channel, before the final dipole magnet. The electrons and some muons in the beam were rejected in this coincidence by the timing between $S1$ and rf. The remaining muon contamination (about 1%) was measured by the time of flight of the particles down the beamline. The spacial and rate stability of the beam was also monitored 3 m downstream of the target by counting particles scattered at 30° from an aluminum target. During the experiment a multiwire proportional chamber was used to monitor the beam position and profile 1.4 m upstream of the target. The pion flux during the data taking was typically 1.3×10^6/s and the momentum spread was 1% $\Delta p/p$.

A CD_2 target of 0.445 g/cm thickness and greater than 0.99% isotopic purity was used. Background events from the carbon were measured with a carbon target of 0.314 g/cm^2 thickness. The energy losses of the particles in the CD_2 and carbon targets were therefore well matched. The thicknesses of the targets are known to an accuracy of 2%. A CH_2 target was used to provide an absolute time calibration using the πp elastic scattering reaction.

The detection system, illustrated in Fig. 2, consisted of six pion scintillation telescopes, 1 m from the target, and six proton telescopes, 1.3 m from the target. The solid angles of the pion and proton telescopes were 29.6 and 23.5 msr, respectively, and the angular acceptances were 5.8° and 4.4°, respectively. The proton telescopes were placed at angles corresponding to the recoil proton angles from quasifree πp scattering for each of the six pion telescopes. The electronics for the experiment was arranged such that each pion telescope was in coincidence with each of the proton telescopes. Therefore 36 pion-proton angle pairs were recorded simultaneously. An event was defined as a coincidence between any pion-proton coincidence and BEAM (defined above). Each telescope consisted of two scintillators, one of which was viewed by a photomultiplier at each end in order to provide better timing resolution. The timing resolution obtained for the proton-pion TOF difference was better than 0.5 ns. This corresponds to a momentum resolution of better than 10 MeV/c at low proton momenta and a resolution of 30 MeV/c in the worst cases at high proton momenta.

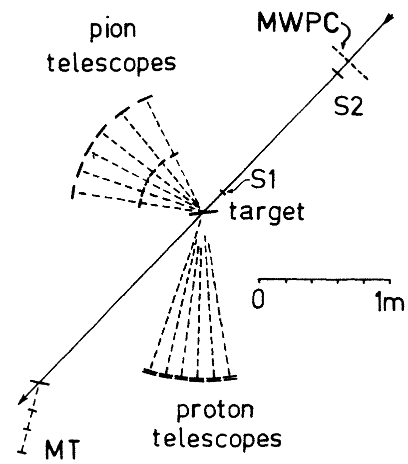

FIG. 2. Schematic drawing of the time-of-flight spectrometer, showing the incident pion counters ($S1$,$S2$), the multiwire proportional chamber (MWPC), an independent beam monitor telescope (MT), and the pion and proton telescopes.

The effect of multiple pions in the same cyclotron beam burst (counted as one pion in the beam definition) was measured by generating events using a separate electronic circuit (where BEAM was delayed in the event definition by the beam pulse repetition time, 20 ns). These events were recorded throughout the data taking and amounted to 10% of the normal events. The data were corrected accordingly. The reliability of the circuit was tested by measuring cross sections at beam intensities from 4.0×10^5 to 2.1×10^6 pions per second. The corrected data were all consistent within a statistical uncertainty of 2%.

IV. DATA ANALYSIS

Proton momenta were determined from the p-π TOF difference. Using this difference has the advantage that at high proton momenta (low pion momenta), where the proton TOF does not change very much with energy, the pion TOF is sensitive to the proton momentum. Energy losses of the pion and proton in the target (through half the target thickness) and through the air were taken into account in calculating the proton momenta. The effects of the finite target thickness and timing resolution on the momentum distributions were calculated with a Monte-Carlo program, discussed later.

The foreground and the background from carbon (properly normalized to the foreground) are displayed in Fig. 3. As one can see, in the regions far away from the quasifree πp kinematics the background counting rate from the carbon was larger than that from the deuterium. This background, coming mostly from (π,π'p) processes, is smooth. Although good statistics were obtained from the carbon target, the background contributed significantly to the uncertainties of the data points where the πd breakup cross section is low. An extra contribution was added to the error bars of the cross section results to account for the 3%

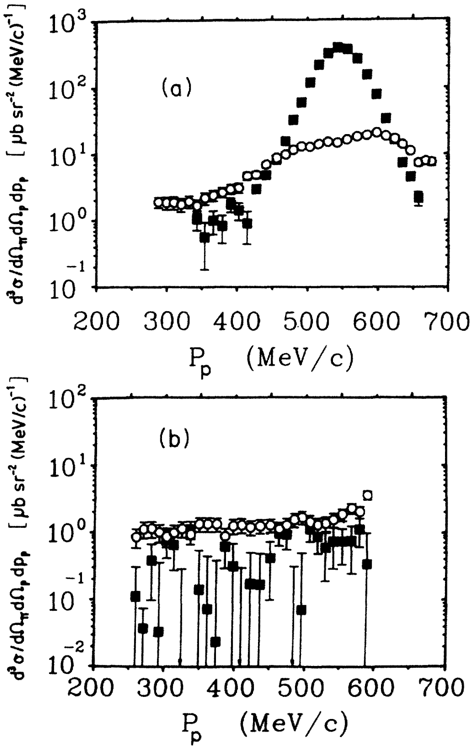

FIG. 3. Differential cross section for the reaction $\pi^+d\to\pi^+pn$ (full squares) and the background from carbon (open circles) at $T_\pi=228$ MeV. The background shown is the differential cross section, measured with the carbon target, divided by two to compensate for the ratio of carbon to deuterium nuclei in CD_2. The spectra in (a) are at detector angles corresponding to quasifree πp kinematics ($\theta_\pi=106.5°$, $\theta_p=-27.9°$) and (b) is far away from quasifree kinematics ($\theta_\pi=106.5°$, $\theta_p=52.6°$).

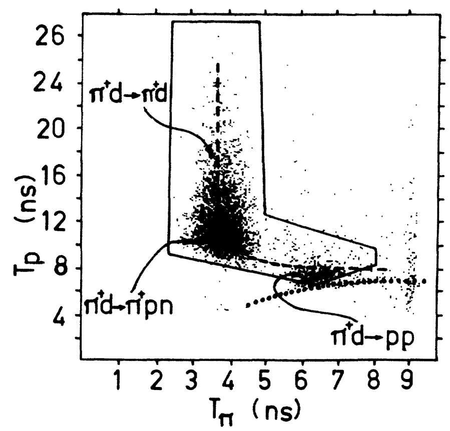

FIG. 4. Density plot of events from the CD_2 target showing a polygonal cut made on the proton versus pion time of flight. The dashed line shows the locus of events from the $\pi^+d\to\pi^+pn$ reaction and the dotted line shows the locus from this reaction where the pion is detected with the proton telescope and the proton with the pion telescope. Events from the $\pi^+d\to\pi^0pp$ reaction are beyond the right-hand side of the figure.

uncertainty in the relative thicknesses of the CD_2 and carbon targets.

Background may also arise from πd elastic scattering, absorption, and charge exchange reactions on the deuterium and also from reversed events, where the pion is detected by the proton telescope and the proton by the pion telescope. In order to ensure that no events from these contaminant reactions survived in the analysis, other cuts were made on the data. These included a two-dimensional cut in the pion TOF and proton TOF shown in Fig. 4. For those angle pairs where two-body final state reactions (πd elastic scattering and absorption) are kinematically allowed, the range of proton momenta were restricted in order to exclude contributions from these reactions. The loci of these reactions are shown in Fig. 4 although the elastic scattering is not evident in the data.

The cross sections are given by:

$$\frac{d^3\sigma}{d\Omega_\pi d\Omega_p dP_p}=\frac{\text{Yield}}{N_{\text{beam}}N_{\text{tgt}}\epsilon\Delta\Omega_\pi\Delta\Omega_p\Delta P_p},$$

where N_{beam} is the number of incident pions; N_{tgt} is the areal density of deuterons in the target; ϵ is the combined efficiency of the detectors and the data acquisition system (varying between 0.7 and 0.9); $\Delta\Omega_\pi$ and $\Delta\Omega_p$ are the pion and proton telescope solid angles (29.6 and 23.5 msr, respectively); and Δp_p is the proton momentum bite (10 MeV/c).

The measured cross sections are the averages over the angular acceptance of the detectors and the momentum

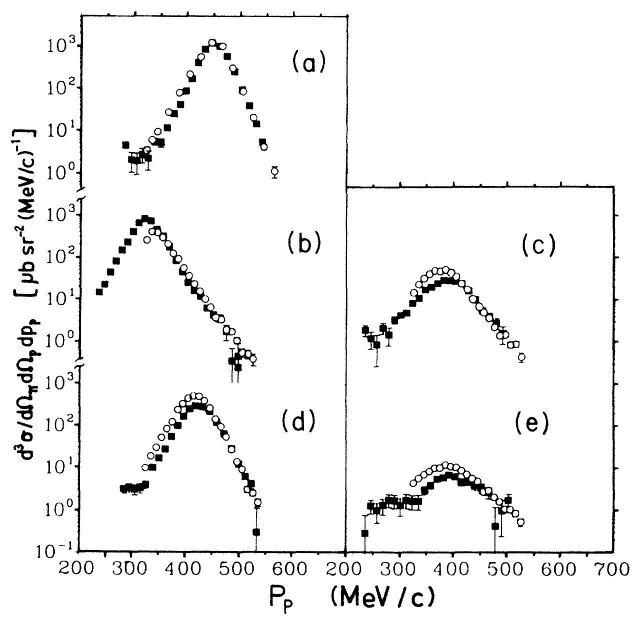

FIG. 5. Differential cross sections measured at $T_\pi=228$ MeV here (solid squares) compared to those measured by Hoftiezer *et al.* (Ref. 20) (open circles). The data of Hoftiezer *et al.* were interpolated, using the polynomial fit described in the text, to angles equal to those of the present work. The pion and proton angles (θ_π and θ_p) and the original angles of the Hoftiezer data (θ'_π and θ'_p) are ($\theta_\pi,\theta_p;\theta'_\pi,\theta'_p$): (a) 106.5°, −27.9°; 105.0°, −30.0°, (b) 61.6°, −50.0°; 60.0°, −50.0°, (c) 85.0°, −50.0°; 85.0°, −50.0°, (d) 95.0°, −37.8°; 95.0°, −40.0°, (e) 95.0°, −50.0°; 95.0°, −50.0°.

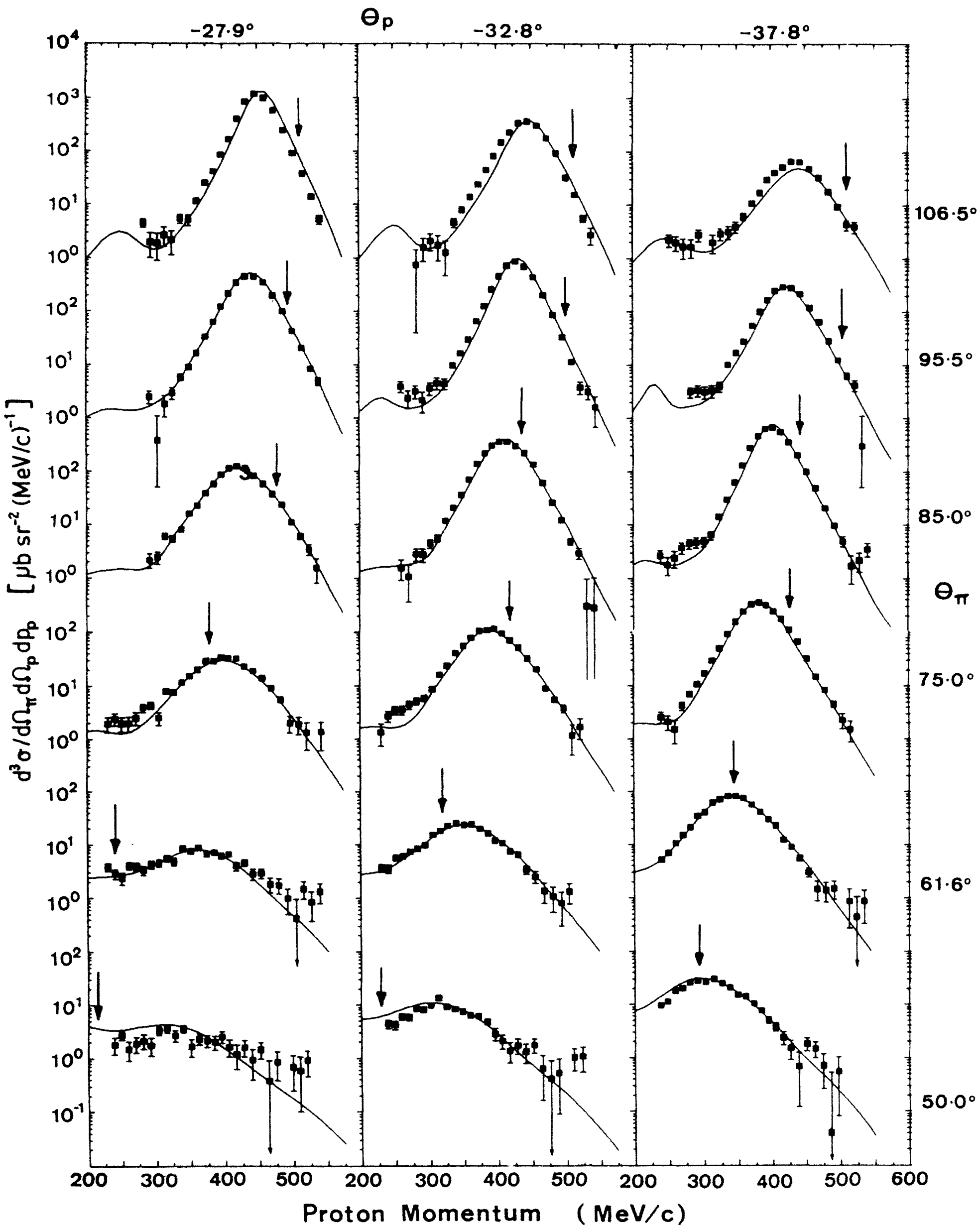

FIG. 6. Comparison of the experimental data at $T = 228$ MeV with the calculations described in the text. The positions where the πp invariant mass is equal to the Δ^{++} mass are indicated by arrows.

binning of the data. Since the cross sections vary nonlinearly with proton momentum and pion and proton angles this average is not equal to the cross section at the center of the acceptance. The data were corrected for this effect, since it is not realistic to average a complex theoretical calculation over the experimental acceptance for comparison with the data. This deconvolution was performed with a Monte-Carlo simulation of the experiment, including the effects of energy loss, multiple scattering, pion decay, and timing resolution. At each energy the cross sections were first fitted with a polynomial which gave a good representation of the distribution of the cross sections over the whole range of angles and momenta. This polynomial was then used as input for a Monte-Carlo program which calculated the average of the cross section distribution over the acceptance of each data point. The ratio of this average and the polynomial value at the center of acceptance of the data point was used to correct for the finite acceptance. In principle this process should be iterated, but it was found that the first step in the iteration was adequate. This procedure had the effect of raising the heights of the peaks by about 20% and lowering the sides of the peaks by about 20%. Approximately 2% statistics were accumulated in the Monte Carlo averaging for each data point. The statistical uncertainties of the Monte-Carlo averages were added in quad-

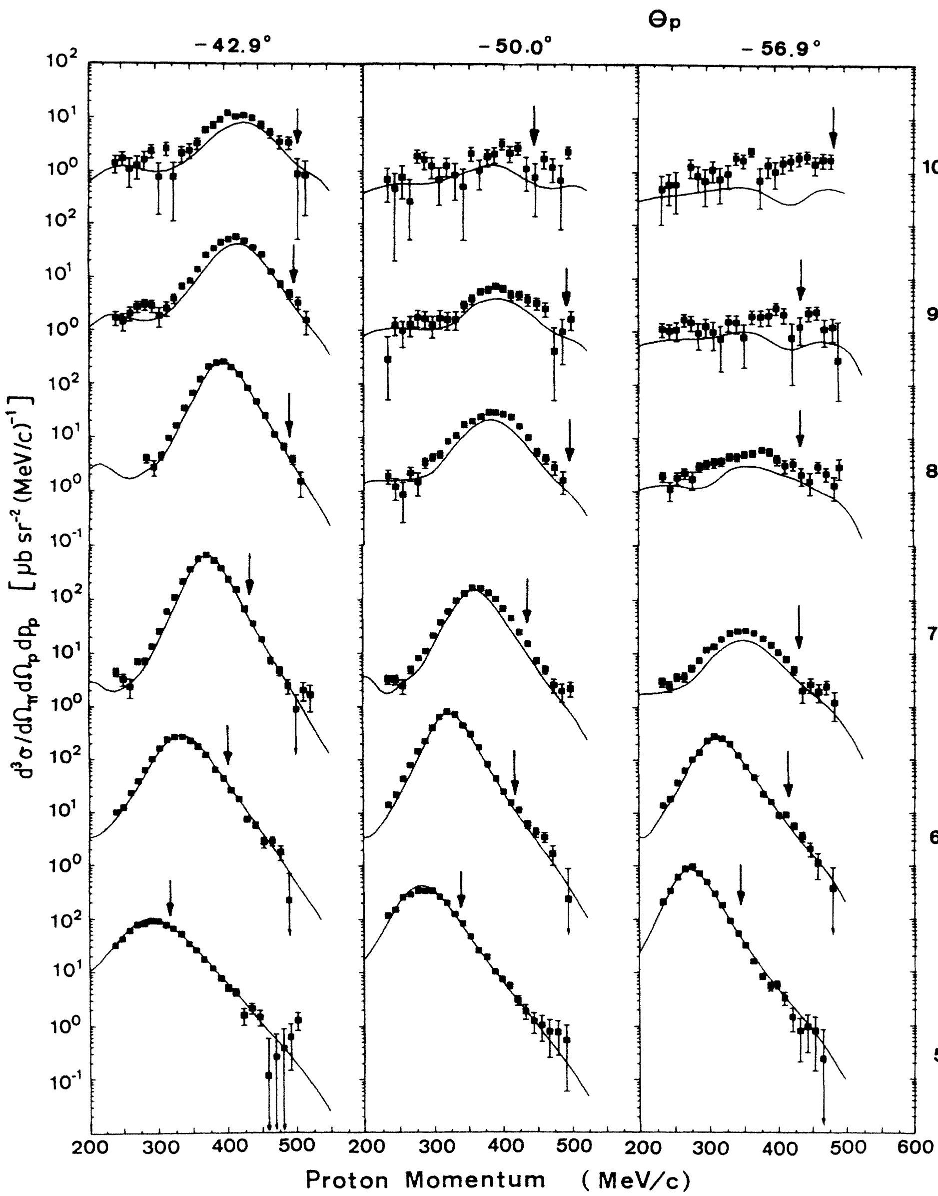

FIG. 7. The same as Fig. 6 at larger proton angles.

rature to the errors of the data points.

It is estimated that systematic uncertainties in the data (not included in the error bars) add to 10%. These arise from the Monte-Carlo corrections (5%), beam flux normalization (1%), CD_2 target thickness (2%), and the solid angles of the two detectors (1% each).

V. RESULTS AND DISCUSSION

Momentum distributions of the protons from the $\pi^+d \rightarrow \pi^+pn$ reaction have been obtained between 250 and 650 MeV/c for 36 pairs of proton and pion angles at 228 MeV and 56 angle pairs at 294 MeV incident pion energy. This large number of data cannot be presented in numerical form in this paper, but may be obtained from the authors. In Fig. 5 we compare the threefold differential cross sections from this experiment (at $T_\pi = 228$ MeV) with the published results of Hoftiezer *et al.*[20] at several angles. The data of Hoftiezer *et al.* were interpolated, using the polynomial fit mentioned above, to angles corresponding to those in this experiment. The greatest change in angle was 2.2°. There is good agreement in the region of large proton momenta, but for smaller momenta there are large discrepancies, which may be related to some acceptance problems of the magnetic spectrometer which was used to measure proton momenta in the experiment of Hoftiezer *et al.*

The complete set of our data is displayed in Figs. 6 and 7, and 8 and 9. For most of the angular pairs one observes approximately Gaussian-shaped momentum distributions. There are three regions of particular interest:

(1) The first is at the location of the maxima in the

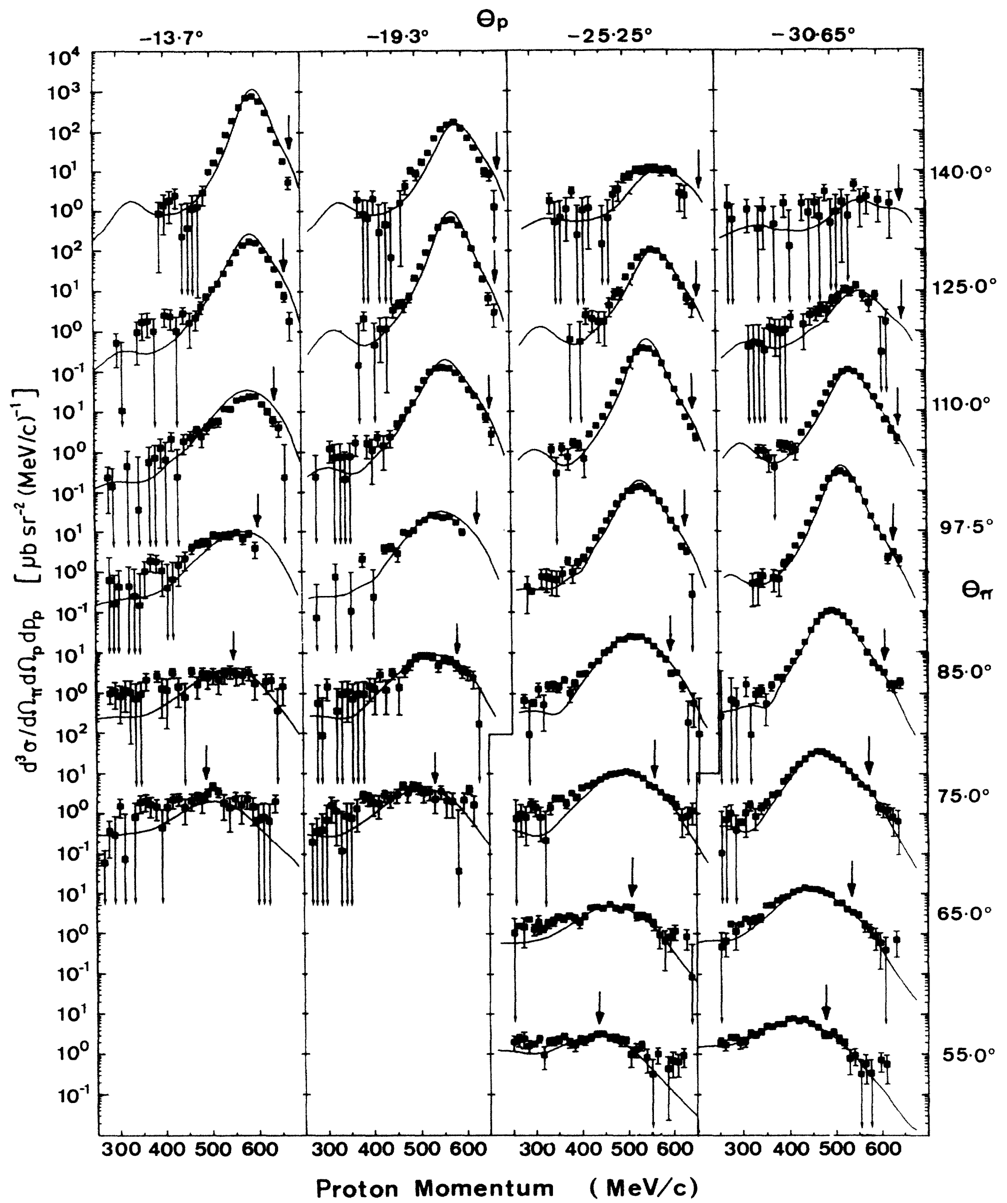

FIG. 8. Comparison of the experimental data at $T_\pi = 294$ MeV with calculations described in the text. The positions where the πp invariant mass is equal to the Δ^{++} mass are indicated by arrows.

cross sections (corresponding to smallest neutron momenta.) The maxima of those distributions which lie on the diagonal line from the upper left to the lower right corner of Figs. 6 and 7, and 8 and 9 correspond to zero neutron momentum (the quasifree πp scattering process). On both sides of these momentum distributions one rapidly departs from the quasifree kinematics.

(2) The second region of interest is the part of the momentum distribution at low momentum. There pn final state interactions dominate and some tailing off from the rapid decrease of the cross sections is observed.

(3) The third region is the place where the mass of the π^+p subsystem is close to the Δ^{++} mass. Generally it is located at larger proton momenta and is indicated by vertical arrows. Within the accuracy of our data no significant enhancements in the cross sections are observed there, although small structures (changes in the shape of the cross section) may exist.

The extensive data from this measurement are compared with the calculations (described in Sec. II), shown as solid lines in the figures. There is a spectacular agreement with the shape and absolute magnitudes of the momentum distributions for the vast majority of the data. Variations of the cross sections over three orders of magnitude are reproduced. In the Δ^{++} regions only very small enhancements of the cross section are predicted in some momentum distributions. They are too small to be recognized in the figures. This small effect of the Δ^{++} formation on the cross section is explained by the fact that the dominant factor in the $\pi^+d \rightarrow \pi^+pn$ reaction is the deuteron

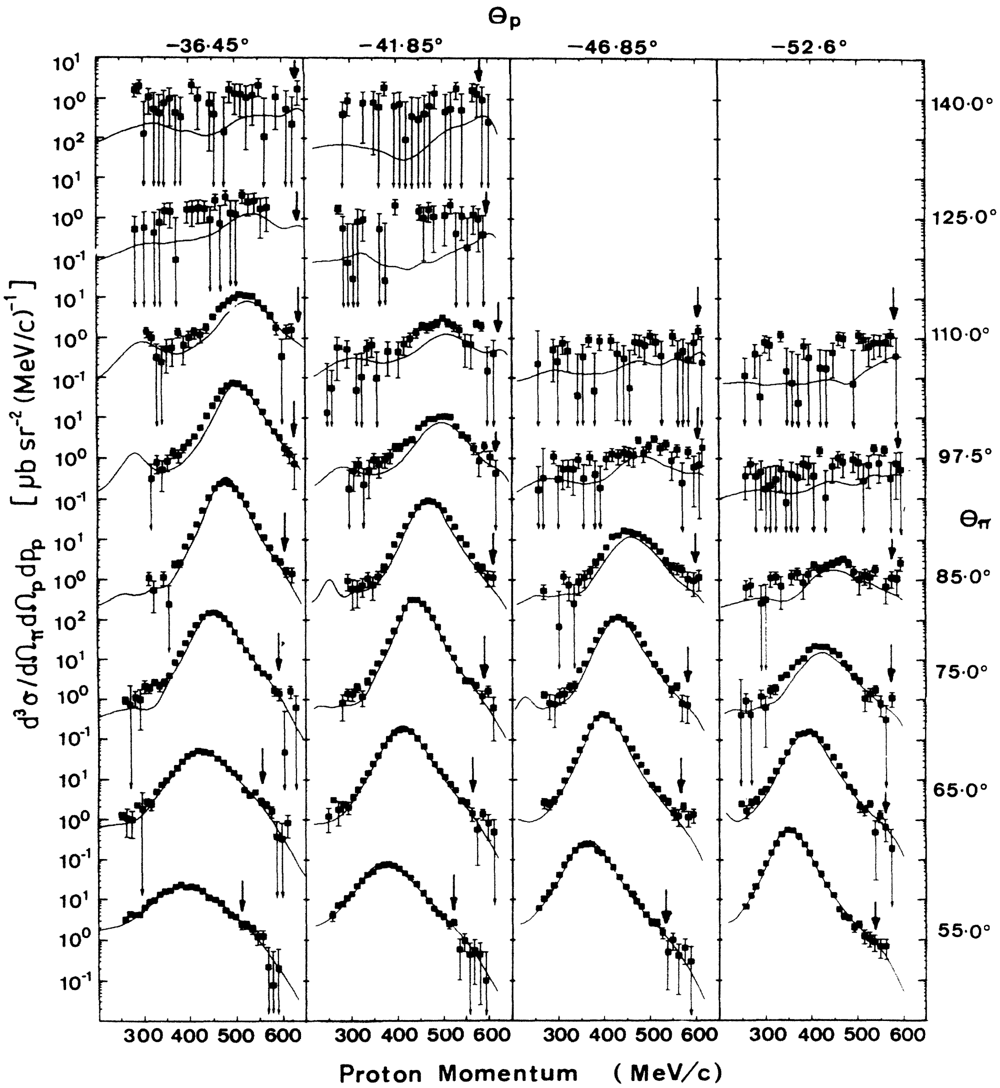

FIG. 9. The same as Fig. 8 at larger proton angles.

form factor, which is rapidly varying as a function of momentum. This is strikingly different from the inelastic reaction $pp \to \pi^+ pn$ where the cross section[16,17] is dominated by the Δ^{++} production.

As to the remarkable agreement between the bulk of the experimental data and the theoretical calculation, one should emphasize that the theoretical predictions (containing no free parameters) are from the same calculation which successfully predicts the differential cross section,[7] vector analyzing power,[8] and the tensor polarization data of Ungricht *et al.*[10] in the πd elastic channel. With such good agreement between conventional theory and experiment there appears to be little room for exotic effects like dibaryon resonances. It is possible, however, that spin averaged observables, like the differential cross section presented here are not sensitive enough to detect dibaryon signals. A more sensitive test of the relativistic Faddeev theory is provided by measurements of the vector analyzing power iT_{11} which are discussed in the following paper.

ACKNOWLEDGMENTS

This work would have been impossible without the generous help and the considerable skills of the staff of SIN. This work was supported by the Bundesministerium für Forschung und Technologie of the Federal Republic of Germany.

*Permanent address: Escuela Superior de Física y Matemáticas, Instituto Politécnico Nacional, México 14, D.F., Mexico.

†Present address: University of Regina, Regina, Saskatchewan, Canada S4S 0A2.

‡Present address: TRIUMF, Vancouver, British Columbia, Canada V6T 2A3.

[1]J. Bystricky and F. Lehar, Fachinformationszentrum, Karlsruhe report 11-1—3, 1978 (unpublished).

[2]D. V. Bugg, *The Interaction between Medium Energy Nucleons in Nuclei—1982 (Indiana University),* Proceedings of the Workshop on the Interaction Between Medium Energy Nucleons in Nuclei, AIP Conf. Proc. No. 97, edited by H. O. Meyer (AIP, New York, 1982), p. 1.
[3]D. V. Bugg, Proceedings of the 10th International Conference on Few Body Problems in Physics, Karlsruhe, 1983, Nucl. Phys. **A416**, 227c (1984).
[4]N. Hiroshige *et al.*, Prog. Theor. Phys. **72**, 1446 (1984).
[5]K. Gabathuler *et al.*, Nucl. Phys. **A350**, 253 (1980).
[6]R. C. Minehart *et al.*, Phys. Rev. Lett. **46**, 1185 (1981).
[7]C. R. Ottermann *et al.*, Phys. Rev. C **32**, 928 (1985).
[8]G. R. Smith *et al.*, Phys. Rev. C **29**, 2206 (1984).
[9]E. Ungricht *et al.*, Phys. Rev. Lett. **52**, 333 (1984).
[10]E. Ungricht *et al.*, Phys. Rev. C **31**, 934 (1985).
[11]W. Grüebler *et al.*, Phys. Rev. Lett. **49**, 444 (1982).
[12]W. König *et al.*, J. Phys. **69**, 2211 (1983).
[13]F. Shimizu *et al.*, Nucl. Phys. **A386**, 571 (1982).
[14]L. G. Dakhno *et al.*, Phys. Lett. **B114**, 409 (1982).
[15]M. M. Calkin, Ph.D. thesis, Rice University, 1984 (unpublished).
[16]A. D. Hancock *et al.*, Phys. Rev. C **27**, 2742 (1983).
[17]J. Hudomalj-Gabitzsch *et al.*, Phys. Rev. C **18**, 2666 (1978).
[18]R. Shypit *et al.*, Phys. Lett. **B124**, 314 (1983).
[19]J. H. Hoftiezer *et al.*, Phys. Lett. **88B**, 73 (1979).
[20]J. H. Hoftiezer *et al.*, Phys. Rev. C **23**, 407 (1981).
[21]For the theoretical development see Refs. 18—43 in, G. R. Smith *et al.*, Phys. Rev. C **29**, 2206 (1984).
[22]W. Grein, A. König, P. Kroll, M. P. Locher, and A. Svarč, Ann Phys. (N.Y.) **153**, 30 (1984).
[23]M. P. Locher and A. Svarč, J. Phys. G **11**, 183 (1985).
[24]W. Jauch, A. König, and P. Kroll, University of Wuppertal Report WU B84-7, 1984.
[25]M. Araki, Y. Koike, and T. Ueda, Prog. Theor. Phys. **63**, 2133 (1980).
[26]I. Duck and E. Umland, Phys. Lett. **96B**, 230 (1980).
[27]W. Grein, K. Kubodera, and M. P. Locher, Nucl. Phys. **A356**, 269 (1981).
[28]Yu. D. Bayukov *et al.*, Yad. Fiz. **20**, 59 (1974) [Sov. J. Nucl. Phys. **20**, 30 (1975)].
[29]Yu. D. Bayukov *et al.*, Nucl. Phys. **A282**, 389 (1977).
[30]L. G. Dakhno *et al.*, Pis'ma Zh. Eksp. Teor. Fiz. **30**, 467 (1979) [JETP Lett. **30**, 43 (1979)].
[31]L. G. Dakhno *et al.*, Yad. Fiz. **31**, 630 (1980) [Sov. J. Nucl. Phys. **31**, 328 (1980)].
[32]L. G. Dakhno *et al.*, Pis'ma Zh. Eksp. Teor. Fiz. **34**, 296 (1981) [JETP Lett. **34**, 283 (1981)].
[33]L. G. Dakhno *et al.*, Phys. Lett. **123B**, 33 (1983).
[34]L. G. Dakhno *et al.*, Nucl. Phys. **A414**, 477 (1984).
[35]A. Matsuyama, Nucl. Phys. **A379**, 415 (1982).
[36]H. Garcilazo, Phys. Rev. Lett. **48**, 577 (1982).
[37]F. Goetz *et al.*, Phys. Rev. C **31**, 1563 (1985).
[38]E. L. Mathie *et al.*, Phys. Lett. **154B**, 28 (1985).
[39]R. Blankenbecler and R. Sugar, Phys. Rev. **142**, 1051 (1966).
[40]V. A. Alessandrini and R. L. Omnes, Phys. Rev. **139**, B167 (1965).
[41]D. Z. Freedman, C. Lovelace, and J. M. Namyslowsky, Nuovo Cimento **43A**, 258 (1966).
[42]R. Aaron, R. D. Amado, and J. E. Young, Phys. Rev. **174**, 2022 (1968).
[43]W. M. Kloet, R. R. Silbar, R. Aaron, and R. D. Amado, Phys. Rev. Lett. **39**, 1643 (1977).
[44]W. M. Kloet and R. R. Silbar, Nucl. Phys. **A338**, 281 (1980).
[45]R. R. Silbar and W. M. Kloet, Nucl. Phys. **A338**, 317 (1980).
[46]W. M. Kloet and R. R. Silbar, Phys. Rev. Lett. **45**, 970 (1980).
[47]V. B. Mandelzweig, H. Garcilazo, and J. M. Eisenberg, Nucl. Phys. **A256**, 461 (1976).
[48]A. S. Rinat and A. W. Thomas, Nucl. Phys. **A282**, 365 (1977).
[49]J. M. Rivera and H. Garcilazo, Nucl. Phys. **A285**, 505 (1977).
[50]R. M. Woloshyn, E. J. Moniz, and R. Aaron, Phys. Rev. C **13**, 286 (1979).
[51]A. S. Rinat, E. Hammel, Y. Starkand, and A. W. Thomas, Nucl. Phys. **A329**, 285 (1979).
[52]N. Giraud, G. H. Lamot, and J. C. Fayard, Phys. Rev. Lett. **40**, 438 (1978).
[53]H. Garcilazo, Phys. Rev. Lett. **45**, 780 (1980).
[54]T. Mizutani and D. S. Koltun, Ann. Phys. (N.Y.) **109**, 1 (1977).
[55]Y. Avishai and T. Mizutani, Nucl. Phys. **A326**, 352 (1979); **A338**, 377 (1980); **A352**, 399 (1981); Phys. Rev. C **27**, 312 (1983).
[56]B. Blankleider and I. R. Afnan, Phys. Rev. C **24**, 1572 (1981).
[57]A. S. Rinat, E. Hammel, Y. Starkand, and A. W. Thomas, Nucl. Phys. **A329**, 285 (1975); A. S. Rinat and Y. Starkand, *ibid.* **A397**, 381 (1983).
[58]C. Fayard, G. H. Lamot, and T. Mizutani, Phys. Rev. Lett. **45**, 524 (1980).
[59]H. Garcilazo, Phys. Rev. Lett. **53**, 652 (1984).
[60]H. Garcilazo, Nucl. Phys. **A360**, 411 (1981).
[61]M. Lacombe *et al.*, Phys. Rev. C **21**, 861 (1980).
[62]M. Lacombe *et al.*, Phys. Lett. **101B**, 139 (1981).
[63]S. Galster *et al.*, Nucl. Phys. **B32**, 221 (1971) and references cited therein.
[64]G. C. Wick, Ann. Phys. (N.Y.) **18**, 65 (1962).
[65]P. B. Bussey *et al.*, Nucl. Phys. **B58**, 363 (1973).